LUND UNIVERSITY

Influence of laser phase and frequency fluctuations on photon-echo data erasure

Elman, U.; Luo, B.; Kröll, Stefan

[Link to publication](#)

Total number of authors:
3

Influence of laser phase and frequency fluctuations on photon-echo data erasure

U. Elman, Baozhu Luo, and S. Kröll

Department of Physics, Lund Institute of Technology (LTH), Box 118, S-221 00 Lund, Sweden

Erasure of data stored by use of photon echoes has been investigated as a function of data writing time and data storage time. The results clarify the requirements on laser phase and frequency stability for performing photon-echo data erasure. The analysis of phase and frequency stability of a light source by the photon-echo erasure process is illustrated. A theoretical analysis emphasizing the physical processes that affect the erasure efficiency as well as an extensive discussion of possible error sources are given. Finally, an approach to bit-selective photon-echo data erasure that is insensitive to laser phase and frequency fluctuations is suggested. © 1996 Optical Society of America.

1. INTRODUCTION

The development of frequency-selective optical memories[1,2] has received increasing attention recently; see, e.g., Refs. 3–5. Spectacular storage densities of >1 Tbit/cm^2 (Ref. 6) and bit rates of $>$Tbits/s (Ref. 7) have been projected and achieved[8] for these types of memory. Frequency-selective optical memories are based on materials with inhomogeneously broadened absorption lines and, in particular, on the property that it is possible selectively to address a large number of different frequency packets within such an absorption line in these materials. A population change induced by a light beam in any specific frequency interval within the absorption line can later be probed and detected. In this way a bit of information has been stored in the sample. The storage time is then determined by the time that it takes the population to decay back into the original state. At liquid-helium temperatures there are many materials for which the number of frequency intervals that can be separately addressed within an inhomogeneous absorption line is very large, $>10^6$.[9,10] The interest in these types of memory arises largely because this number of bits can, in principle, be stored at a single spatial location, yielding an exceptionally large storage density. However, these techniques have other unique features, especially concerning optical processing and manipulation of temporal light sequences.[11–15]

There are two approaches to frequency-selective optical memories: Data can be written and read out in the time or the frequency domain. In the frequency-domain approach the light is simply tuned to the frequency interval where the next data bit is to be written or read. In the time-domain approach[2] an arbitrary sequence of temporal data is sent into the material. For any input data sequence the number of excited atoms in each frequency interval will be proportional to the power spectrum of the input signal at precisely this frequency interval. Assume that the temporal electromagnetic input data field $E_d(t)$ has the temporal Fourier transform $E_d(\omega)$. When an encoded input sequence $E_d(\omega)$ is preceded by a preparation

pulse $E_p(\omega)$, the spectral distribution of excited atoms will be proportional to $|E_d(\omega)+E_p(\omega)|^2$, provided that the homogeneous dephasing time of the transition is much larger than the duration of the sequences and the time between the sequences.[16,17] From the above expression it is clear that the number of excited atoms at any frequency will depend on the relative phase between the two pulse sequences at this particular frequency. If the preparation pulse has a bandwidth equal to or larger than the data sequence bandwidth and a well-defined and known phase at these frequencies, the effective outcome of the excitation process will be that the complete electromagnetic-field Fourier transform of the input data sequence, including the phase, has been stored in the atomic population. The physical mechanism used in the time-domain approach is the photon echo,[2] and hereafter we refer to this approach as time-domain optical storage (TDOS). Among the features demonstrated for TDOS are storage of multiple images at the same spatial location,[3] phase-conjugate storage and readout,[18] temporal correlation,[11] high-density storage,[19] image processing and correlation,[20] and logical processing.[12] In this paper we investigate a bit-selective all-optical concept for erasing data stored by the TDOS technique.

Erasing and rewriting data are desirable and important requirements for the photon-echo storage technique as for any other data storage technique. At one time the erasure techniques that had been considered for the photon-echo and spectral-hole-burning storage techniques were not selective in the sense that it was not possible to erase a single bit in a spatial location while retaining other bits of information at the same spatial address. A process to overcome this difficulty in the case of TDOS was proposed by Akhmediev,[21] who suggested one could erase data bits by rewriting the original data sequence into the material with a phase shift of 180 deg. The conceptual idea is shown in Fig. 1. Figure 1a shows a conventional stimulated echo, in which the population grating set up by the write pulse (w) and the data pulse (d) is probed by the read pulse (r), yielding an output signal time τ after the read pulse. Figure 1b shows the prin-
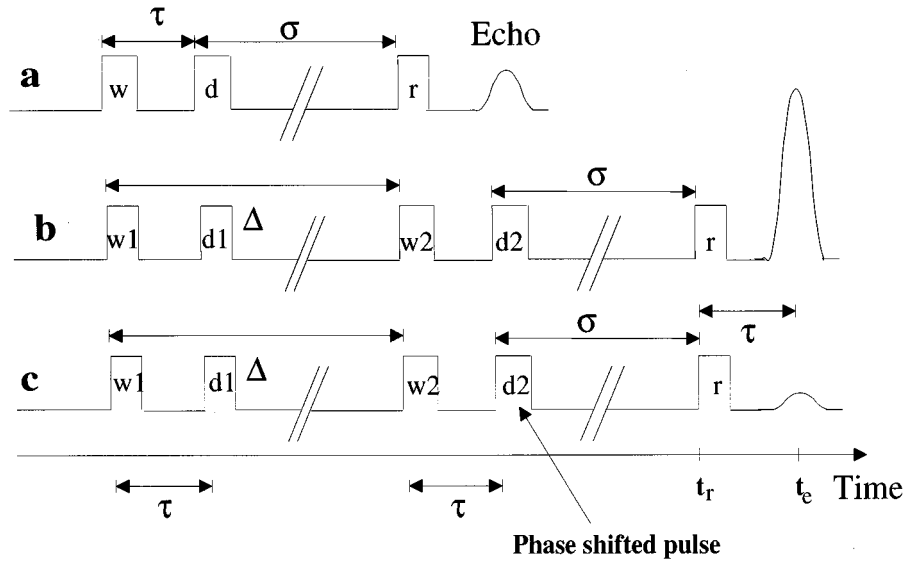
Fig. 1. Typical input sequences for photon-echo experiments together with the definition of the time intervals τ, Δ, and σ used subsequently in this paper. a, the first two pulses write (w), and data (d) create a frequency-dependent population grating in the material, which is probed by the read pulse (r). b, By use of several pairs of write and data pulses the population grating by each pair can be added to the population grating created by the previous pairs, leading to an enhanced signal after readout. c, Phase-shifted data pulse in the second pair. The first and the second gratings cancel instead of enhancing each other, which leads to a suppressed or even an eliminated signal.

ciple of the accumulated photon echo,[22] in which the population grating from a first pulse pair (w1, d1) is enhanced by a second pulse pair (w2, d2), yielding an enhanced echo signal. Finally, Fig. 1c shows the implementation of Akhmediev's erasure concept, in which the phase of one of the pulses, in this case d2, has been shifted such that the population grating set up by the second pair will be out of phase and cancel the effect of the grating set up by the first pair. This figure also shows the symbols used to denote the timing among the pulses, τ, Δ, and σ. These letters are used in the rest of the paper.

Akhmediev's erasure concept was experimentally demonstrated previously by two groups of researchers using pulsed laser systems.[23,24] In the research presented in this paper a more extensive treatment and analysis of this erasure method is given. Using amplitude-modulated collinear continuous-wave excitation has yielded better control of the individual excitation pulses. It has therefore been possible to study the erasure efficiency as a function, e.g., of storage time and pulse separation. A discussion of how the performance of the laser system and the physical processes in the storage material affect the erasure efficiency is now given. Tchernyshyov[25] has shown that Akhmediev's erasure method may put insurmountable requirements on the laser stability. Some aspects of this are verified in our measurements but, maybe even more importantly, a novel approach that could eliminate these stringent requirements derived by Tchernyshyov is also presented.

Finally in this introduction, two additional aspects of the present research are mentioned. First, coherent erasure of photon echoes is also a way of experimentally performing all-optical NOT or XOR operations on binary data. These logical operations complement the logical AND and OR operations that we performed earlier.[12] Inasmuch as

one of the pairs of operations AND and NOT or OR and NOT is sufficient for performing any arbitrary logical operation, a complete set of Boolean operations using photon echoes has now been implemented experimentally. Second, one can use measurements of photon-echo erasure efficiencies to determine the phase and the frequency stability of a laser system. This is interesting because some of the liquid-helium-cooled rare-earth-ion-doped crystals that are used as storage materials possess very narrow homogeneous line widths [less than a kilohertz (Ref. 10)] and laser phase drifts of a fraction of a radian can be detected on time scales corresponding to the inverse line width.

A brief theoretical introduction of Akhmediev's concept of coherent erasure in TDOS is given in Section 2. An account of the theoretical background, which includes a more in-depth treatment of the effect of the statistics of the laser phase and frequency fluctuations, is given elsewhere.[26] Section 3 describes the experimental setup, and Section 4 describes the measurements that have been performed. An account of how the laser stability can be inferred from the erasure efficiency and a discussion of some of the approximations in the theoretical description are presented in Section 5. An improvement of the present concept for coherent erasure in TDOS is also put forward in that section. Section 6 contains a brief summary of our results.

2. THEORY

The conventional stimulated photon echo is a generalized four-wave mixing process in which the excitation pulses arrive at the sample at different times. The output electromagnetic field $E_{out}(t)$ from a time-ordered process such as that in Fig. 1a can (assuming that the pulses do not

saturate the transition) be written as

$$E_{out}(t) \propto \int_{-\infty}^{\infty} E_w{}^*(\omega)E_d(\omega)E_r(\omega)\exp(i\omega t)\mathrm{d}\omega \qquad (1)$$

(Ref. 27), where $E_w(\omega)$, $E_d(\omega)$, and $E_r(\omega)$ are the frequency Fourier transforms of the time-dependent input-pulse electromagnetic fields. With more than three input pulses (as in Figs. 1b and 1c) higher-order processes can occur, but if we limit ourselves to third-order processes any combination of three pulses will generate an output pulse by an expression similar to the one above. If several third-order processes generate output fields that occur at the same time (as in Figs. 1b and 1c) the individual output fields from the different processes should be added coherently.[22] In particular, we are interested in the output at time $t_e = t_r + \tau$, which can be expressed as

$$E_{out}(t) \propto \int_{-\infty}^{\infty} [E_{w1}{}^*(\omega)E_{d1}(\omega)$$
$$+ E_{w2}{}^*E_{d2}(\omega)]E_r(\omega)\exp(i\omega t)\mathrm{d}\omega. \qquad (2)$$

To simplify the algebra we assume that the excitation pulses have a Fourier-limited band width and a Gaussian temporal profile and that all have the same peak amplitude. Thus the input electromagnetic fields are represented as

$$E_k(t) = E_0 \exp\left[-2\left(\frac{t - t_k}{T}\right)^2 - i(\omega_k t + \phi_k)\right], \qquad (3)$$

with Fourier transforms

$$E_k(\omega) = E \exp\left\{-\frac{[T(\omega + \omega_k)]^2}{8}\right\}\exp\{-i[(\omega+\omega_k)t_k$$
$$+ \phi_k]\}. \qquad (4)$$

It is clear from relation (2) and Eq. (4) that, if all input pulses have the same duration T, frequency ω_k, and phase relations $(\phi_{w1} - \phi_{d1}) = (\phi_{w2} - \phi_{d2}) + \pi$, then $E_{out}(t)$ will be zero. In this way, applying the pair w2 and d2 eliminates the stimulated output from pulses w1 and d1. If all excitation pulses are emitted from a perfectly frequency-stabilized light source, then $\phi_{w1} = \phi_{d1} = \phi_{w2} = \phi_{d2}$. In this case, by adding an externally controlled phase shift ϕ_{ext} to one of the write or data pulses one may choose to remove or enhance the information stored by the first pair by letting ϕ_{ext} take the value π or 0, respectively. In several of the experimental results presented in the paper the quantity $\eta = $ (output signal when $\phi_{ext} = 0$)/(output signal when $\phi_{ext} = \pi$) is measured. This quantity will be called the erasure efficiency. When $\phi_{w1} = \phi_{d1} = \phi_{w2} = \phi_{d2}$ and the frequencies of all pulses are the same, then η is infinite; and when the above phases all are completely random η will approach unity. To interpret and discuss the experimental results it will be helpful to understand how the erasure efficiency depends on the phases and frequencies of the excitation pulses. These will therefore now be explicitly calculated. The phase will be allowed to take an arbitrary value, and the frequency during the first pulse pair, which will be denoted ω_1, will be allowed to be different from the frequency of the other three pulses, ω_2. The time between the two pulses within a pulse pair is, however, assumed to

be so short that the frequency shift during this time can be neglected. Clearly more general cases can be treated, but this choice of parameters is adequate for discussing our experimental data. The output field E_{out} for each of the two terms in relation (2) will be calculated separately and then added coherently. From relation (2) and Eq. (4) we obtain E_{out}(pair 1) as

$$E_{out}(t) = C \exp\left\{-\frac{[T(\omega_1 - \omega_2)]^2}{12}\right\}\exp\left[-\frac{2}{3}\left(\frac{t - t_e}{T}\right)^2\right]$$
$$\times \text{(phase factor)}. \qquad (5)$$

Thus the output field is a Gaussian pulse centered at time t_e (see Fig. 1). The constant C depends on, e.g., the number density and the electric dipole moment of the absorbers, the length of the active medium, and the input-pulse amplitude and duration but not on the input-pulse frequencies, phases, or time separations. As can be seen, the amplitude of this output field decreases as a function of the frequency difference between the input pulses. This reduction takes place because the readout pulse at frequency ω_2 does not address exactly the specific frequency interval near ω_1 where the input grating was engraved. Adding the output from the second pulse pair, w2 and d2 (Fig. 1), and that assuming the phase of, e.g., the second input pulse in the first pair, d1, has been shifted by an external phase shift ϕ_{ext} give a total output intensity

$$I_{out}(t) = |E_{out}(\text{pair } 1)\exp(-i\phi_{ext}) + E_{out}(\text{pair } 2)|^2$$
$$\propto \exp\left[-\frac{4}{3}\left(\frac{t - t_e}{T}\right)^2\right]\{1 + e^{-2\gamma} + 2e^{-\gamma}$$
$$\times \cos[\Delta\phi - \phi_{ext} + 2(\omega_1 - \omega_2)(t - t_e)/3]\}, \qquad (6)$$

where

$$\gamma = \frac{[T(\omega_1 - \omega_2)]^2}{12}, \qquad (7)$$

$$\Delta\phi = (\omega_1 - \omega_2)\tau + (\phi_{w1} - \phi_{d1}) - (\phi_{w2} - \phi_{d2}). \qquad (8)$$

In the present experiments the integrated signal S is measured. Integrating I_{out} in relation (6) over time finally yields

$$S \propto 1 + e^{-2\gamma} + 2e^{-2\gamma} \cos(\Delta\phi - \phi_{ext}). \qquad (9)$$

Thus the erasure efficiency finally becomes

$$\eta = \frac{S(\phi_{ext} = 0)}{S(\phi_{ext} = \pi)} = \frac{1 + e^{-2\gamma} + 2e^{-2\gamma} \cos(\Delta\phi)}{1 + e^{-2\gamma} - 2e^{-2\gamma} \cos(\Delta\phi)}. \qquad (10)$$

As can be seen from Eq. (10), the erasure efficiency is the highest if all pulses have equal frequency and $\cos(\Delta\phi) = 1$. If the pulses have equal frequency the last condition says that, whatever phase shift occurs between the pulses in the first pulse pair, a complete erasure of the stored data can still occur as long as an exactly identical phase shift takes place between the two pulses in the second pair. The calculations in this section include several approximations. Some of these are discussed in Section 5.

3. EXPERIMENT

The experimental setup is shown in Fig. 2. A Spectra-Physics SP171 argon-ion laser is pumping a Coherent Radiation CR699-21 ring dye laser. The excitation pulses are created from the continuous-wave dye laser output beam by two Isomet 1205C acousto-optic modulators. Not only could these modulators be used for amplitude modulation, but with their Model D322B drivers we could also impose a frequency shift on the excitation beams by changing the frequency of the acoustic wave in the modulators. A Gsänger LM 0202 electro-optic modulator is configured such that it can shift the phase of the incoming light π rad without changing the polarization or intensity of the light. The electronic timing was controlled mainly through four Stanford Research System DG135 delay generator cards inserted in a personal computer. The laser light is tuned to the $^3H_4 - {}^1D_2$ transition at $\lambda = 611$ nm and focused with a 15-cm lens onto a 1-mm-thick 0.1% Pr^{3+}-doped $YAlO_3$ crystal inside a liquid-helium bath cryostat (the temperature is normally 4.2 K). Some relevant data for this crystal and transition can be found in Ref.
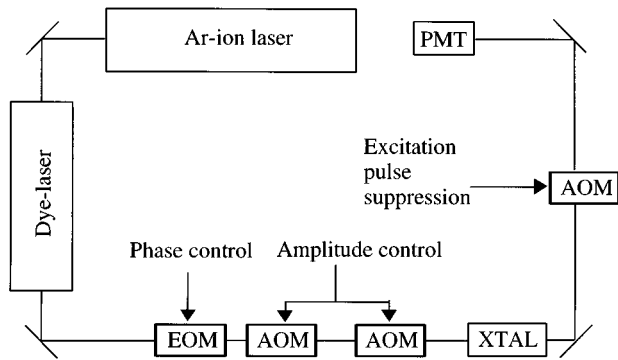

Fig. 2. Experimental set up: EOM, electro-optic modulator; AOM is acousto-optic modulators; XTAL, crystal; PMT, photo-multiplier tube.
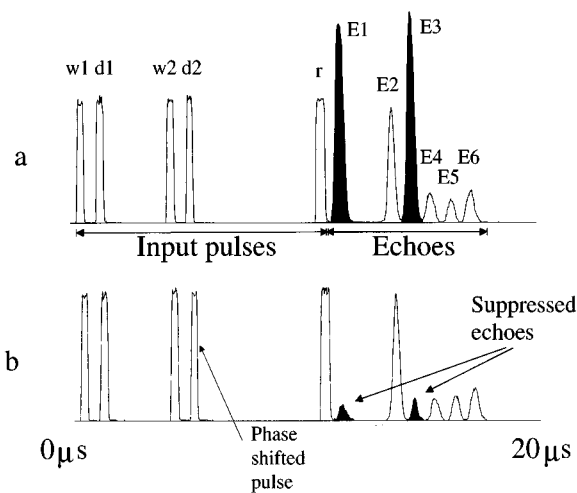

Fig. 3. Experimental recordings of pulse sequences corresponding to a, Fig. 1b and b, Fig. 1c. The notation for the excitation pulses is the same as in Fig. 1. There are several echo output pulses, denoted E1–E6. As can be seen, not only one but two of the echo output pulses are suppressed when a phase shift is applied. Further discussion is given in the text.

28. A third acousto-optic modulator is used after the crystal to suppress the transmitted input pulses, which are temporally separated from the echo output pulses. Finally, the light is detected by a photomultiplier tube. An example from an oscilloscope recording of the photo-multiplier tube output from a pulse sequence for investigating the echo-suppression efficiency is shown in Fig. 3. The two pulse pairs and the readout pulse are applied to the sample, and, as is seen, there are several echo output pulses. Pulses E1–E4 are stimulated echoes, and pulses E5 and E6 are two-pulse echoes. The electromagnetic fields of the stimulated echoes depend on the input-pulse amplitudes and phases. Echo E1 is created from the pulse combinations $(w1 \times d1 + w2 \times d2) \times r$. E2 is generated by the sequence $d1 \times w2 \times r$, E3 by $(w1 \times w2 + d1 \times d2) \times r$, and E4 by $w1 \times d2 \times r$. The photon-echo outputs for Figs. 3a and 3b differ because in Fig. 3b the electro-optic modulator introduces a 180-deg phase shift during the last input pulse, d2. It is clear from the figure that not only echo E1 but also echo E3 is erased. That both echoes are erased can be understood from the above description of which combinations of input pulses generate the different echoes. Figure 3 also illustrates that the erasure effect can be incomplete (meaning that the echo output signal is not exactly zero after the erasure process). This fact is discussed in some detail below.

4. MEASUREMENTS

In this project our intention has been to clarify to what extent stored data can be erased by coherent addition of a new excitation-pulse sequence. Because, in practice, data could be erased only when the time between the write pulse and the data pulse was quite short (<1–2 μs), a data sequence consisting of only a single data pulse was employed. The erasure efficiency η was then investigated as a function of the time separation τ between the write and the data pulses (see Fig. 1) and as a function of the time separation between the pulse pairs, Δ. In addition the results from these measurements caused us to calibrate and check our measurements by deliberately introducing known phase and frequency changes into our excitation pulses to verify our understanding of the processes that were taking place. Figure 4 shows the erasure efficiency versus pulse separation τ. Here Δ is 10 μs, σ is 7 μs (see Fig. 1), and the duration of each pulse is 100 ns. {The specified pulse lengths are always full widths at half-maximum, which equals $T^* \sqrt{[\ln(2)]} \approx T/1.2$.} It is clear from Fig. 4 that the erasure efficiency decreases rapidly as a function of pulse separation. We interpret this as an effect of the random phase fluctuations of the laser source, which occur between the first and the second pulses in each pulse pair. This is a plausible explanation considering that commercial continuous-wave dye lasers are known to exhibit random phase shifts of the order of radians in a few microseconds; see, e.g., Ref. 29. A consequence of this explanation is that the erasure data also can be used to infer the laser phase drift versus time, as discussed below. The suggestion that the erasure process is incomplete because of random phase shifts was also made credible by an experiment in which deliberate and controlled phase shifts ϕ_{ext}
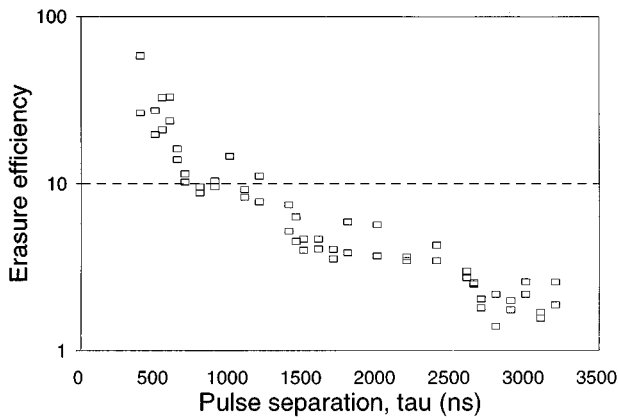
Fig. 4. Erasure efficiency, as defined in the text, versus the temporal separation between the write and data pulses (τ) in each pair. The rapid decrease of the erasure efficiency as a function of the pulse separation is interpreted as being caused by laser phase fluctuations.
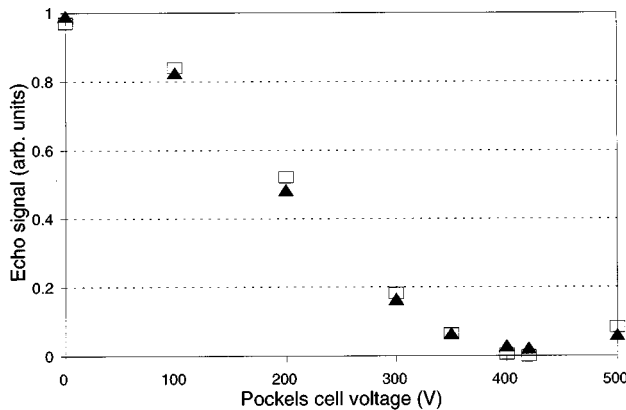

Fig. 5. Echo signal for two accumulated excitation pulse pairs versus Pockels cell voltage applied to the electro-optic modulator in Fig. 2. For zero voltage the excitation sequence corresponds to that in Fig. 1b. The electro-optic modulator voltage for 180-deg phase shift is ~420 V. At this voltage the excitation sequence corresponds to the trace in Fig. 1c. Good agreement is obtained between experimental (▲) and theoretical (□) values.

different from π were introduced by the electro-optic modulator. Figure 5 shows the experimental erasure efficiencies together with the theoretical values calculated from Eq. (10). As can be seen, the agreement is good.

A more careful inspection of Fig. 4 shows that the erasure efficiency exhibits a modulation as a function of pulse separation. This is ascribed to the intensity modulation that occurs for photon echoes in Pr:YAlO$_3$ when the excitation pulses are so short that the corresponding Fourier frequency bandwidth is larger than the separation between the upper-state hyperfine levels.[30] When a superposition of the upper-state hyperfine components is excited, the signal strength of the stimulated photon echo is a strongly modulated function both of the separation between the first and second pulses and of the separation between the second and third pulses. Although in this experiment the separation between the first and second pulses is the same for both pulse pairs, the time to the third pulse, the readout pulse, is different for the two pairs. The amplitudes of the frequency gratings from the

first and the second pairs will therefore normally not be the same, and there will be a residual frequency-dependent population distribution that adds to other effects that make the erasure process incomplete.

Figure 6 shows the erasure efficiency versus the time separation between the two pulse pairs, Δ. The pulse duration is 200 ns, σ is 500 μs, and the pulse separation within each pair, τ, is 500 ns (filled triangles) and 1000 ns (open triangles). For these measurements it is important that the time between the second and third pulses, σ, be long enough that the upper-state populations have decayed. The decrease in erasure efficiency that occurs because the upper-state population from the first pair has had more time to decay than the population from the second pair is discussed in Subsection 5.B. A decrease in erasure efficiency as σ is decreased has been observed for large Δ, as expected. For the τ-dependence experiments with small Δ, as in Fig. 4, a σ dependence neither is expected nor has been observed. In Fig. 6 the erasure efficiency continuously drops as a function of the pulse pair separation, although this occurs on a much slower time scale than in Fig. 4. Based on relation (6) and Eq. (8) it is reasonable to assume that the decrease of the erasure efficiency in Fig. 6 is caused by longer-term laser frequency drifts, mainly through the term $(\omega_1 - \omega_2)\tau$ in Eq. (8). The effect of the pure phase term $(\phi_{w1} - \phi_{d1}) - (\phi_{w2} - \phi_{d2})$ in the expression for $\Delta\phi$ seen in Fig. 4 can also be seen in Fig. 6 as τ is increased from 500 to 1000 ns. Again, to test our understanding of the processes, two experiments were carried out. First, a five-pulse input sequence as in Fig. 1b was employed. During the first pulse pair the frequency was shifted by the acousto-optic modulators. In this way the term $(\omega_1 - \omega_2)\tau$ in relation (8) could be verified. The experimental conditions were as follows: $T = 1.2 \times 200$ ns, $\tau = 400$ ns, $\Delta = 3$ μs, and $\sigma = 10$ μs. The theoretical expression is given here by relation (9) with $\phi_{ext} = 0$. Figure 7 shows the experimental as well as a theoretical curve for which the value of γ in relation (9) has been decreased to fit the de-
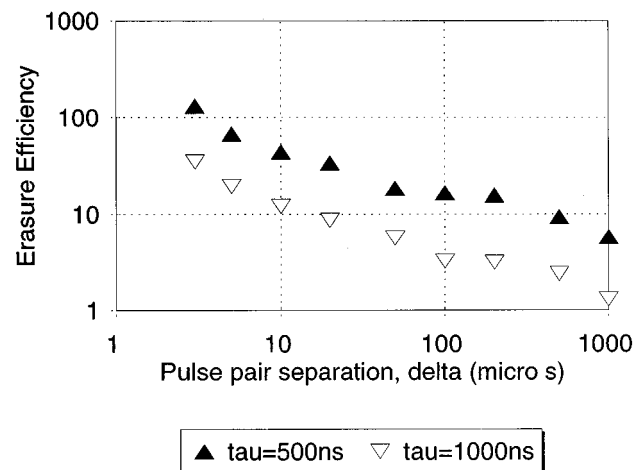

Fig. 6. Erasure efficiency, as defined in the text, versus the separation between the two excitation pulse pairs for two different separations between the pulses within a pair (▲, 500 ns and ▽, 1000 ns). The decrease in erasure efficiency as a function of pulse pair separation is interpreted as being caused by laser frequency drift.
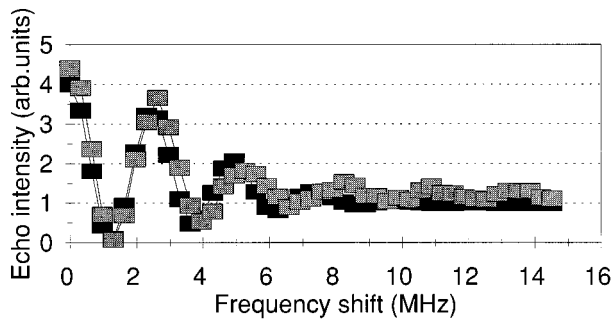
Fig. 7.   Echo intensity for an excitation sequence as in Fig. 1b as a function of frequency shift applied to the first excitation pulse pair. Darker figures, theory; lighter figures, experiment.
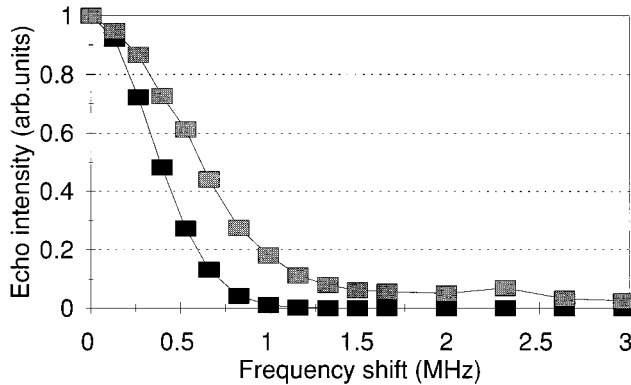

Fig. 8.   Echo intensity for an excitation sequence as in Fig. 1a as function of frequency shift applied to the third pulse, r. Darker figures, theory; lighter figures, experiment.

cay of the oscillations. As can be seen, good agreement is obtained for the sinusoidal oscillations that arise from the term $(\omega_1 - \omega_2)\tau$ in Eq. (8), indicating that we have understood the process that decreases the erasure efficiency in Fig. 6. However, as the theoretical oscillations decreased more rapidly than the experimental data, stimulated echoes (Fig. 1a), in which a deliberate frequency shift was introduced during the third pulse, were performed. The pulse duration was 700 ns. The relative echo size I_{echo} is plotted in Fig. 8 together with the theoretical curve, $I_{echo} = \exp[-(\Delta\omega T)^2/6]$, as a function of frequency shift $\Delta\omega = 2\pi\Delta\nu$. We obtain the theoretical curve simply by taking the square of Eq. (5) (integration over the duration of the echo pulse will not affect the frequency-shift dependence). In this experiment it is possible to study separately the influence of a decay term $\exp(-2\gamma)$ of a type identical to that which appears in relation (9). As can be seen, the experimental decay is too slow; as a matter a fact, the discrepancy between experiment and theory increases when the pulse duration is decreased. The reason for this discrepancy is not known to us. The hump in the experimental curve close to 2.4 MHz probably occurs because the frequency shift here is close to the separation between the highest and lowest hyperfine levels in the upper state. Hyperfine effects can possibly explain why the experimental curve drops less rapidly than the theoretical as a function of frequency shift. Such hyperfine effects could also increase in importance when the excitation pulses get shorter, because this would increase their spec-

tral band widths and make them more efficient in populating several hyperfine levels simultaneously.

5. DISCUSSION

A. Inferring the Laser Phase and Frequency Stability from the Erasure Efficiency

From Eq. (10) and Section 2 it is seen that the erasure efficiency can decrease either because the average frequency during the first excitation pulse pair is different from the average frequency during the second excitation pulse pair (through the quantity γ) or because the accumulated phase of the excitation light between the two pulses in the first pair is different from the accumulated phase between the two pulses in the second pair (described as $\Delta\phi$). These quantities are related but not equivalent. The γ parameter depends not strictly on the frequencies between the pulses in the pulse pair but only on the light frequency during the pulses. The accumulated phase clearly depends on the frequency between the pulses. So the light frequency during all pulses can be exactly the same, but if there is some kind of phase jump between the two pulses in one of the pairs the erasure efficiency still can be low. On the other hand, the accumulated phase between the first and second pulses can be the same in the first and second pairs, but if the frequencies during the pulses in the pairs are different the erasure will still be incomplete. A consequence of this is that complete erasure cannot be obtained by frequency shifting the light source. Instead the light source has to be phase shifted, and the frequency must remain the same. Mathematically the effects above are also taken into account in Eq. (8) by the separation of the phase shift into a frequency-shift part $\Delta\omega$ and a pure phase-shift part $\Delta\phi_{phase} = (\phi_{w1} - \phi_{d1}) - (\phi_{w2} - \phi_{d2})$.

Because the above separation of the total accumulated phase shift $\Delta\phi$ into two is only a conceptual construction in part, the two terms are not strictly independent. (A more rigorous statistical analysis of this situation is given in Ref. 26.) However, assuming that the two contributions $\Delta\omega$ and $\Delta\phi_{phase}$ can be treated as independent and separate entities, one can arrive at the conclusion that the frequency shift should depend mainly on the time between the two pulse pairs, whereas the pure phase-shift part should depend mainly on the time between the pulses within the pair. The last statement follows from the fact that the phase-shift part is due to random events (typically thickness fluctuations in the dye jet) that take place during the time interval within the pulse pairs, whereas the frequency drift within the 1-MHz dye laser bandwidth of the ring dye laser locking system occurs over longer time scales. That such a frequency drift indeed exists over time scales of and near 100 μs can be seen, e.g., in Ref. 31. It can then be reasonable to describe the pure phase term $\Delta\phi_{phase}(\tau) = (\phi_{w1} - \phi_{d1}) - (\phi_{w1} - \phi_{d2})$ as a function of the pulse separation τ and the frequency shift $\Delta\omega$ as a function of the pulse pair separation Δ. The experiments performed in this research are designed to show the behavior of specifically these two contributions. Figure 4, the τ dependence, illustrates mainly the pure phase term $\Delta\phi_{phase}(\tau)$. Because the two pulse pairs are close to each other in time
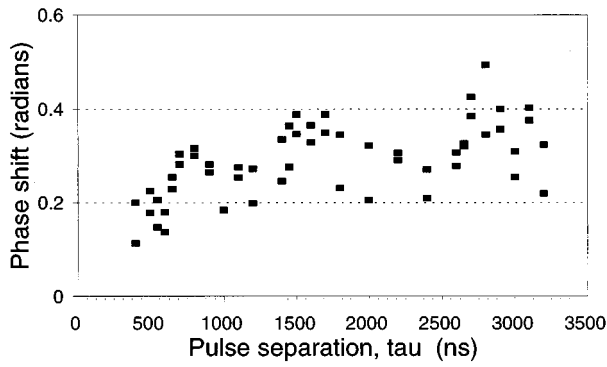
Fig. 9.   Laser phase shift versus time as calculated from the experimental data in Fig. 4.   As discussed in the text, a laser frequency drift of 40 kHz during 10 μs has been assumed in addition to the phase shift.

(10-μs separation) it is reasonable to assume that the frequency shift $\Delta\omega(10\ \mu s) = 2\pi\Delta\nu(10\ \mu s)$ is small.   From Fig. 6 one can calculate complementary values of $\Delta\nu(3\ \mu s)$ ($\Delta\nu$ at $\Delta = 3\ \mu s$) and $\Delta\phi_{phase}$ using Eq. (10). Assuming that $\Delta\phi_{phase} = 0$ at $\Delta = 3\ \mu s$, one obtains $\Delta\nu(3\ \mu s) = 55$ kHz. Assuming instead that $\Delta\nu(3\ \mu s) = 0$, one obtains $\Delta\phi_{phase} = 0.17$. $\Delta\phi_{phase} = 0$ and $\Delta\phi_{phase} = 0.17$ give $\Delta\nu = \Delta\nu(10\mu s) = 94$ kHz and $\Delta\nu = \Delta\nu(10\ \mu s) = 40$ kHz, respectively.   Somewhat arbitrarily we choose $\Delta\nu$ to be equal to 40 kHz and use this in our subsequent analysis. If this is the case we can calculate the accumulated phase difference versus τ, $\Delta\phi_{phase}(\tau)$, for the two pulse pairs from the experimental results in Fig. 4 by inverting Eq. (10). If the phase drift during the second pair and the phase drift during the first pair are independent we get the total phase shift, on average, by adding these two individual shifts in quadrature.   As the shifts can be assumed to be of equal size, the laser phase drift versus time is $\Delta\phi_{phase}(\tau)/(\sqrt{2})$.   This quantity is plotted in Fig. 9, versus the pulse separation (τ).   Figure 10 shows the experimental value of $\Delta\nu(\Delta)$ that we obtained from the experimental data of Fig. 6 by inverting Eq. (10).   To obtain $\Delta\nu(\Delta)$ it is necessary to have a value for the quantity $\Delta\phi_{phase}(\tau)$. This value is calculated for $\tau = 500$ and $\tau = 1000$ ns for $\Delta = 10\ \mu s$ with $\Delta\nu = 40$ kHz.   As can be seen, the calculated values for $\Delta\nu$ appear to be independent of τ, as they should be according to our assumptions.   The drift $\Delta\nu$ occurs because acoustical vibrations and jet thickness fluctuations cause the laser frequency to change.   Because of the limited bandwidth of the servo system and the relatively low-finesse reference cavity the laser frequency will not return exactly to its previous value.   However, as can be seen from Fig. 10, the drift is significantly smaller than 1 MHz, which is the line width specified for the Coherent CR699-21 system.

Through the parameter γ in Eq. (10) it can also be seen that the erasure efficiency will depend on the pulse duration.   As can be concluded from the discussion in connection with Eq. (5), the factors $\exp(-2\gamma)$ describe the effect that the first and second excitation pairs physically address different frequency intervals.   Narrow-band excitation pulses (corresponding to a long duration assuming Fourier width limited pulses) would therefore be more susceptible to this effect, as is mathematically manifested through the product $\Delta\omega T$ in Eq. (7).   The erasure effi-

ciency should consequently be slightly less for long pulses than for short pulses.   The effect is, however, rather small.   Taking the largest value $\Delta\nu = 200$ kHz from Fig. 10 still gives only $\exp(-2\gamma) \approx 0.99$ ($T = 1.2 \times 200$ ns). In our measurements this effect is negligible.   But in principle the effect of pulse duration could be observed for longer pulses or larger shifts.

Because of the phase and frequency sensitivity it seems clear that the erasure efficiency can be a sensitive measurement of the stability of a laser source.   Because there are materials with homogeneous dephasing times longer than milliseconds,[10] the phase stability can be detected down to ~0.1 rad/ms or better, and the long-time frequency stability can be detected with at least kilohertz stability over periods of several hours or even days in rare-earth-ion-doped crystals when one considers that the spectral information engraved by the input pulses is destroyed only by the ultraslow relaxation of the ground-state hyperfine levels.[3,32] Finally, this measurement technique is not restricted to continuous-wave lasers but can equally well be applied to measuring the stability of pulsed lasers, e.g., mode-locked laser systems.

B.   Approximations and Error Sources

There are a variety of approximations done in the model and analysis presented in this paper.   Some of these are discussed and described in this subsection.   In addition to laser phase and frequency fluctuations, erasure efficiency will also be affected by laser amplitude fluctuations, upper-state saturation, excited-state decay, decay of the ground-state hyperfine level population, and delay-time error of the laser pulses.

A calculation shows that the critical quantity in delay-time errors is the ratio between the pulse duration $T/1.2$ and the difference in delay times between the pulses in the two pairs, $\delta = \tau_{second\ pair} - \tau_{first\ pair}$.   If $\delta/T = 0.1$ the maximum erasure efficiency is 600.   Our smallest pulse duration was 100 ns, the rms error of the time delay of the SRS 135 digital delay generator cards was less than 50 ps, and from the experiment we could see that the stability of the time separation between pulses was much better than 10%.   Consequently any influence of delay-
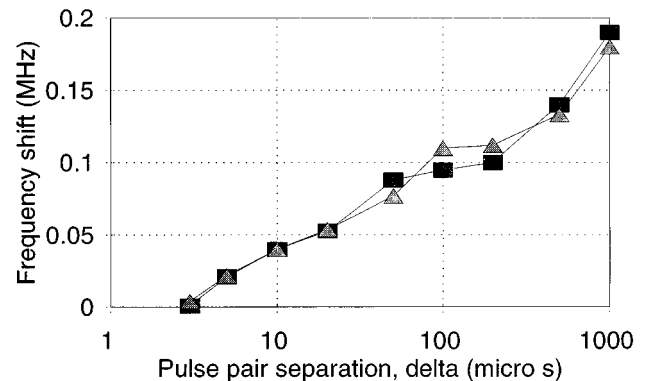

Fig. 10.   Laser frequency drift versus time calculated from the experimental data in Fig. 6 assuming the frequency drift is 40 kHz after 10 μs. Dark rectangles, $\tau = 500$ ns; light triangles, $\tau = 1000$ ns.
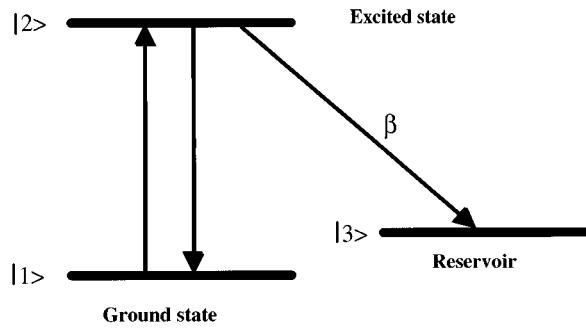
Fig. 11. Schematic energy-level diagram of the energy levels of relevance for the erasure process. $|1\rangle$ is the ground state. The excitation pulses transfer population between states $|1\rangle$ and $|2\rangle$. A fraction β of the atoms present in state $|2\rangle$ after the excitation will decay (radiatively or nonradiatively) to reservoir state $|3\rangle$. After a comparatively long time (0.1–1 s) the atoms will decay from the reservoir state back to the ground state.

time error should be negligible in our measurements.

For time scales shorter than 20 μs the amplitude variation of the input laser radiation is less than 4%. Calculations show that amplitude variations less than 3% lower in one pulse pair than in the other pulse pair give a maximum erasure efficiency of 1000. For longer pulse separations the amplitude stability is still better than 5%, yielding a maximum erasure efficiency of 400. For longer pulse pair separations, bubbles in the liquid-helium bath could affect the relative intensities of the pulse pairs at the crystal. However, no change in the erasure efficiency could be observed when the cryostat was evacuated to the lambda point. The shot-to-shot stability of the echo is, as expected, significantly better below the lambda point than at 4 K.

Another error source was also not included in the analysis: The atoms excited by the light pulses are continuously decaying, and this process affects the erasure efficiency. The essential part of the population transfer process in the system is illustrated in Fig. 11. The first excitation pulse pair will transfer a population proportional to the term $E_{w1}{}^*(\omega)E_{d1}(\omega)$ in relation (2) to the upper state, $|2\rangle$. This population will decay with the time constant T_1, which for Pr-doped YAlO$_3$ is ~180 μs.[28] A fraction β of the decaying atoms will decay to the reservoir state $|3\rangle$. In this case the reservoir state corresponds to a hyperfine level different from the hyperfine level that the ion occupied from the start, i.e., level $|1\rangle$ in Fig. 11. Eventually this fraction β in state $|3\rangle$ will decay back to state $|1\rangle$. For Pr-doped YAlO$_3$ this will occur at a time constant T_R ranging from 0.3 to 1 s at 4 K, depending on the hyperfine level.[33] Assuming that all excitation pulses have identical amplitude and neglecting saturation effects, we can modify the output echo electromagnetic field that is due to the excitation pulses in relation (2) for the upper-state decay as

$$E_{\text{out}}(t) \propto \int_{-\infty}^{\infty} [E_{w1}{}^*(\omega)E_{d1}(\omega)$$
$$\times \exp(-\Delta/T_1) + E_{w2}{}^*(\omega)E_{d2}(\omega)]$$
$$\times \exp(-\sigma/T_1)E_r(\omega)\exp(i\omega t)\mathrm{d}\omega, \qquad (11)$$

where the term $\exp(-\Delta/T_1)$ describes the decay of the upper state between the first and second pulse pairs and the term $\exp(-\sigma/T_1)$ describes the excited-state population decay during the time between the second pulse pair and the readout pulse. Also, expression (11) contains several approximations. Loss of phase coherence between the first and the second pulse in each pair and between the readout pulse and the echo, $\exp(-\tau/T_2)$, where T_2 is the homogeneous dephasing time of the transition, has been neglected. The reason for this is that those terms affect the gratings created by both the first and the second pulse pair in the same way and therefore should not influence the erasure efficiency. Terms of the order of $\exp(-\tau/T_1)$ have been put equal to unity, $\tau \ll T_1$ has been assumed, and this means that the excitation pulses are assumed to be short compared with all relaxation times in the system, which is true in the present experiment. A more rigorous theoretical description of stimulated photon echoes including relaxation processes can be found, e.g., in Ref. 34. Relation (11) can be used to describe the influence of excited-state decay on the τ dependence of the erasure efficiency plotted in Fig. 4. With a Δ of 10 μs we get a maximum erasure efficiency $\eta > 1000$. Thus the time between the pulse pairs is so short that the effect of the upper-state decay has negligible influence on the erasure efficiency. For the Δ dependence the upper-state decay certainly affects the data. In fact, with a σ of 0.5 ms almost all the upper-state atoms have decayed. However, because some of the upper-state atoms decay to the reservoir state, $|3\rangle$, there will be some remaining frequency population distribution in the ground state, $|1\rangle$ in Fig. 11. This remaining frequency distribution will still contribute to an echo signal after all upper-state atoms have decayed. If this is taken into account Eq. (11) is modified as

$$E_{\text{out}}(t) \propto \int_{-\infty}^{\infty} E_{w1}{}^*(\omega)E_{d1}(\omega)[\exp[-(\Delta + \sigma)/T_1]$$
$$+ (\beta/2)\{1-\exp[-(\Delta + \sigma)/T_1]\}]E_r(\omega)$$
$$\times \exp(i\omega t)\mathrm{d}\omega + \int_{-\infty}^{\infty} E_{w2}{}^*(\omega)E_{d2}(\omega)$$
$$\times [\exp(-\sigma/T_1) + (\beta/2)$$
$$\times [1 - \exp(-\sigma/T_1)]]E_r(\omega)\exp(i\omega t)\mathrm{d}\omega.$$
$$(12)$$

The contributions from the first and second pairs have been broken into two separate integrals. The first term in each set of boldface brackets describes the contribution from the remaining upper-state population, and the second term describes the signal contribution for the atoms that have decayed to the reservoir state. The decay from the reservoir state is so slow that it has been neglected for the time scales in our experiments. The factor $\beta/2$ arises because after excitation to the upper state the ground- and upper-state population gratings contribute to the echo signal with equal amounts, but, after the decay of the upper state, only the ground-state grating contributes to the signal, reducing the echo output field a factor of 2. Assuming identical pulse intensities, the maximum erasure efficiency will be

$$\eta = \left(\frac{\exp[-(\Delta + \sigma)/T_1] + (\beta/2)\{1 - \exp[-(\Delta + \sigma)/T_1]\} + \exp(-\sigma/T_1) + (\beta/2)[1 - \exp(-\sigma/T_1)]}{\exp[-(\Delta + \sigma)/T_1] + (\beta/2)\{1 - \exp[-(\Delta + \sigma)/T_1]\} - \exp(-\sigma/T_1) - (\beta/2)[1 - \exp(-\sigma/T_1)]} \right)^2 . \quad (13)$$

Comparing the signal strength for a three-pulse echo with $\sigma = 10$ μs and $\sigma = 1$ ms results in a difference of a factor of ~20 for short separations between the first and second pulses. The signal ratio echo($\sigma = 10$ μs)/echo($\sigma = 1$ ms) $= (\beta/2)^2$ gives a relatively high branching ratio β in the range 0.4–0.5. This value is considerably greater than the theoretical estimation in Ref. 35 but consistent with the results in Ref. 36. With $T_1 = 180$ μs, $\beta = 0.4$, $\sigma = 0.5$ ms, and $\Delta = 1$ ms (the worst case Δ in Fig. 6) we obtain $\eta \approx 90$. Thus the above effect should not significantly affect the data in Fig. 6.

Another effect that has also been neglected throughout the analysis is the nonuniform profile of the inhomogeneous broadening. However, because in this experiment only a few megahertz within a profile with a full width half-maximum of several gigahertz have been used, the initial number of atoms can be assumed to be constant within the megahertz frequency interval used for the storage.

As was pointed out by Akhmediev,[21] the erasure process studied in this paper does not remove the original population grating that is responsible for the storage; instead, a frequency-dependent population grating, phase shifted by 180 deg, is superposed upon the grating created by the previously stored data bit. Assuming that the original data input pulses and the input pulses for erasure have the same intensity, the second grating will cancel the effect of the first grating if the upper- and lower-state population difference is essentially the same when the data enter the sample as when the erasure pulses enter. To get an impression of the degree to which this condition is needed we can, for our case, assume that the data bit pair and the erasure pair will both transfer a fraction ϵ of the ground-state population to the upper level. The first grating will then be based on the fraction ϵ of the total number of atoms. The erasure grating will be created by a fraction ϵ of the remaining ground- and upper-state population difference, i.e., a fraction $\epsilon(1 - 2\epsilon)$ of the original total, where the factor 2 arises because the population transfer in the limit of weak excitation is proportional to the difference between the upper- and lower-state populations. There will thus be a remaining grating buildup by a fraction $2\epsilon^2$ of the atoms. As it is a coherent process, the photon-echo signal is proportional to the number of participating atoms squared, which means that the signal strength of the echo before erasure is proportional to ϵ^2 and the remaining signal after erasure is proportional to $(2\epsilon^2)^2 = 4\epsilon^4$. Throughout this paper we have defined the erasure efficiency as the echo signal for coherent addition of the two pulse pairs divided by the echo signal after erasure. Thus the limitation on the erasure efficiency that is due to population transfer for the above case will be approximately $(2\epsilon)^2/4\epsilon^4 = 1/\epsilon^2$. The effect of the population transfer's causing the population gratings to differ in size has been neglected throughout the paper. However, the experiments have been carried out in what we may call the linear regime. Here this means that the excitation pulses are far from saturating the transition, and therefore one can calculate the effect of consecutive excitation sequences simply by adding their individual effects. For population transfers of a few percent for each pulse pair we see that the effect of the population changes described above is negligible in comparison with the erasure efficiencies that we obtained.

C. Improvements of the Erasure Process

It is clear from the measurements reported here that the requirements on laser stability for efficient coherent erasure are large. An additional complication that has not been discussed occurs if the efficiency in the writing process is large, i.e., the branching ratio β for the upper-state relaxation to the reservoir state is large, which is desirable for photon-echo storage; see, e.g., Ref. 7. If β is large and if the data rate is sufficiently high there will be a buildup of the population in the reservoir state. Even if all excitation pulses are weak, a high pulse rate can cause significant excitation. For the erasure process it is really the excitation processes that have occurred between the writing pulse pair and the erasing pulse pair that are critical. Thus a high upper-state population is no problem *per se*; only changes in the population distribution are a problem. On the other hand, some of the atoms will relax to the reservoir state, and both the writing and the erasing processes will promote ions into this state. If the reservoir is sufficiently long-lived essentially all atoms will end up in the reservoir state, the material will exhibit a strong hole-burning effect, and no more information can be stored in the sample until this state has relaxed. To solve this potential problem an alternative erasure process must be suggested.

We will not solve this problem here, but will suggest a novel approach that can significantly reduce or actually maybe even eliminate the sensitivity of the erasure efficiency to laser phase and amplitude variation. This approach is presented in Fig. 12. The input data sequences arrive from the left. At the time a data sequence, or part of a sequence, is to be erased it is read out. The readout pulse and the part of the echo signal that is to be erased are then transmitted through the fibers that constitute what is called the erasure loop. The echo signal is amplified to some nominal value, the phase of the readout pulse (or, alternatively, the phase of the amplified echo signal) is shifted by 180 deg before the readout pulse, and the echo output again goes into the crystal after the loop. Because of the external phase shift imposed on the readout pulse (or data) in the loop, this new input sequence will now produce a population grating exactly canceling the previous grating, provided that only the level of amplification has been correct. This approach is intrinsically self-correcting and self-compensating for any phase, frequency, or amplitude fluctuations of the input pulses. Schemes of this type can be important in view of the theoretical calculation[25] that demonstrates that a straightforward application of Akhmediev's erasure concept[21] can put insurmountable demands on the laser phase stability.
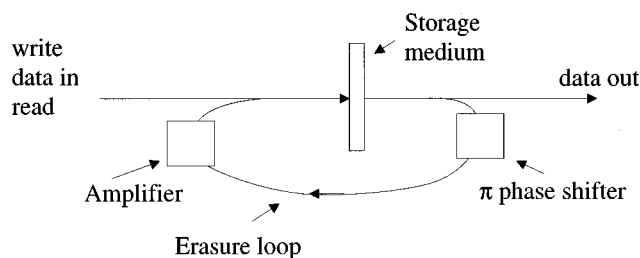
Fig. 12. Conceptual view of how the sensitivity of the erasure process to phase and frequency fluctuations can be eliminated. To erase data stored in the sample the sequence is read out. The read pulse and the output are coupled into the erasure loop where the data sequence is amplified, and the read pulse (or the data sequence) is phase shifted by 180 deg. As they enter the sample again the former read pulse now acts as a write pulse for the recalled data sequence. Because of the added phase shift these input pulses will neutralize the existing population grating from which it was originally generated.

6. SUMMARY

An experimental investigation of all-optical and coherent erasure of data stored by use of photon echoes by retransmitting an identical data pulse phase shifted 180 deg has been presented. A simplified quantitative theoretical analysis has been presented, and error sources and possible refinements of this analysis have been discussed. The analysis describes how the erasure efficiency depends on the phase and frequency stability of the excitation source. The efficiency of the erasure process has been determined experimentally as a function of time separation of the input pulses. These experiments have shown that on the time scale at which most photon-echo data storage experiments are performed today (e.g., see Refs. 11–13 and 16–18) the phase and frequency stability of conventional commercial tunable continuous-wave laser systems is insufficient for achieving a reasonable erasure efficiency. A slightly modified novel erasure approach that is not affected by laser phase and frequency fluctuations has therefore been put forward. Finally we have argued that the types of erasure measurement performed in this study can in principle be used as a diagnostic of the laser phase stability down to levels of a tenth of a radian during a millisecond, or a frequency shift of 1 kHz/h.

REFERENCES

1. W. E. Moerner, *Persistent Spectral Hole-Burning: Science and Applications* (Springer, New York, 1988), Chap. 7, pp. 251–307.
2. T. W. Mossberg, "Time-domain frequency-selective optical data storage," Opt. Lett. **7**, 77 (1982).
3. X. A. Shen, E. Chiang, and R. Kachru, "Time-domain holographic image storage," Opt. Lett. **19**, 1246 (1994).
4. M. Mitsunaga, N. Uesugi, H. Sasaki, and K. Karaki, "Holographic motion picture by Eu^{3+}:Y$_2$SiO$_5$," Opt. Lett. **19**, 752 (1994).
5. E. S. Maniloff, S. B. Altner, S. Bernet, F. R. Graf, A. Renn, and U. P. Wild, "Recording of 6000 holograms by use of spectral hole burning," Appl. Opt. **34**, 4140 (1995).
6. W. R. Babbitt and T. W. Mossberg, "Quasi-two-dimensional time-domain color memories: process limitations and potentials," J. Opt. Soc. Am. B **11**, 1948 (1994).
7. S. Kröll and P. Tidlund, "Recording density limit of photon-echo optical storage with high-speed reading and writing," Appl. Opt. **32**, 7233 (1993).
8. S. Saikan, T. Kishida, A. Imaoka, K. Uchikawa, A. Furusawa, and H. Oosawa, "Optical memory based on heterodyne-detected accumulated photon echoes," Opt. Lett. **14**, 841 (1989).
9. R. Yano, M. Mitsunaga, and N. Uesugi, "Nonlinear laser spectroscopy of Eu^{3+}:Y$_2$SiO$_5$ and its application to time-domain optical memory," J. Opt. Soc. Am. B **9**, 992 (1992).
10. R. W. Equall, Y. Sun, R. L. Cone, and R. M. Macfarlane, "Ultraslow optical dephasing in Eu^{3+}:Y$_2$SiO$_5$," Phys. Rev. Lett. **72**, 2179 (1994).
11. Y. S. Bai, W. R. Babbitt, N. W. Carlsson, and T. W. Mossberg, "Real-time optical waveform convolver/cross correlator," Appl. Phys. Lett. **45**, 714 (1984).
12. S. Kröll and U. Elman, "Photon-echo-based logical processing," Opt. Lett. **18**, 1834 (1993).
13. M. Zhu, W. R. Babbitt, and C. M. Jefferson, "Continuous transient optical processing in a solid," Opt. Lett. **20**, 2514 (1995).
14. W. R. Babbitt and T. W. Mossberg, "Spatial routing of optical beams through time-domain spatial-spectral filtering," Opt. Lett. **20**, 910 (1995).
15. H. Sonajalg, A. Débarre, J.-L. Le Gouët, I. Lorgeré, and P. Tchénio, "Phase-encoding technique in time-domain holography: theoretical estimation," J. Opt. Soc. Am. B **12**, 1448 (1995).
16. W. R. Babbitt, "The response of inhomogeneously broadened absorbers to temporally complex light pulses," Ph.D. dissertation (Harvard University, Cambridge, Mass., 1987).
17. H. Lin, T. Wang, G. A. Wilson, and T. W. Mossberg, "Experimental demonstration of swept-carrier time-domain optical memory," Opt. Lett. **20**, 91 (1995).
18. X. A. Shen and R. Kachru, "Time-domain optical memory for image storage and high-speed image processing," Appl. Opt. **32**, 5810 (1993).
19. H. Lin, T. Wang, and T. W. Mossberg, "Demonstration of 8-Gbit/in.^{2} areal storage density based on swept-carrier frequency-selective optical memory," Opt. Lett. **20**, 1658 (1995).
20. E. Y. Xu, S. Kröll, D. L. Huestis, R. Kachru, and M. K. Kim, "Nanosecond image processing using stimulated photon echoes," Opt. Lett. **15**, 562 (1990).
21. N. N. Akhmediev, "Information erasing in the phenomenon of long-lived photon echo," Opt. Lett. **15**, 1035 (1990).
22. W. H Hesselink and D. A. Wiersma, "Picosecond photon echoes stimulated from an accumulated grating," Phys. Rev. Lett. **43**, 1991 (1979).
23. E. A. Manykin, N. V. Zhamensky, D. V. Marchenko, E. A. Petrenko, and M. A. Selifanov, "Elaboration of rapid data erasure methods in an optical storage device based on the photon echo effect," Opt. Mem. Neural Networks **1**, 239 (1992).
24. M. Arend, E. Block, and S. R. Hartmann, "Random access processing of optical memory by use of photon-echo interference effects," Opt. Lett. **18**, 1789 (1993).
25. O. V. Tchernyshyov, "On coherent erasure of long-lived photon echo," Laser Phys. **2**, 567 (1992).
26. U. Elman and S. Kröll, "Statistical modeling and theoretical analysis of the influence of laser phase fluctuations on photon echo data erasure and stimulated photon echoes," Laser Phys. (to be published).
27. W. R. Babbitt and T. W. Mossberg, "Mixed binary multiplication of optical signals by convolution in an inhomogeneously broadened absorber," Appl. Opt. **25**, 962 (1986).

28. R. M. Macfarlane and R. M. Shelby, "Coherent transient and holeburning spectroscopy of rare earth ions in solids," in *Spectroscopy of Solids Containing Rare Earth Ions*, A. A. Kaplyanskii and R. M. Macfarlane, eds. (Elsevier, New York, 1987), p. 111.

29. J. L. Hall and T. W. Hänsch, "External dye laser frequency stabilizer," Opt. Lett. **9**, 502 (1984).

30. M. Mitsunaga, R. Yano, and N. Uesugi, "Stimulated-photon-echo spectroscopy. II. Echo modulation in Pr^{3+}:$YAlO_3$," Phys. Rev. B **45**, 12760 (1992).

31. A. Szabo and T. Muramoto, "Experimental test of the optical Bloch equations for solids using free-induction decay," Phys. Rev. A **39**, 3992 (1989).

32. M. K. Kim and R. Kachru, "Multiple-bit long-term data storage by backward-stimulated echo in Eu^{3+}:$YAlO_3$," Opt. Lett. **14**, 423 (1989).

33. T. Blasberg and D. Suter, "Nuclear spin relaxation of Pr^{3+} in $YAlO_3$. A temperature-dependent optical-rf double-resonance study," Chem. Phys. Lett. **215**, 668 (1993).

34. M. Mitsunaga and R. G. Brewer, "Generalized perturbation theory of coherent optical emission," Phys. Rev. A **32**, 1605 (1985).

35. L. E. Erickson, "Optical-pumping effects on Raman-heterodyne-detected multipulse rf nuclear-spin-echo decay," Phys. Rev. B **42**, 3789 (1990).

36. Y. S. Bai and R. Kachru, "Spin-fluctuation-induced optical spectral diffusion in Pr^{3+}:$YAlO_3$," Phys. Rev. A **44**, R6990 (1991).